Open access • Journal Article • DOI:10.1088/0953-4075/41/22/225503

Coherent control of magneto-optic rotation — Source link

Kanhaiya Pandey, Ajay D. Wasan, Vasant Natarajan

Institutions: Indian Institute of Technology Roorkee

Published on: 28 Nov 2008 - Journal of Physics B (IOP Publishing)

Topics: Optical rotation, Polarization (waves), Coherent control, Birefringence and Laser

J. Phys. B: At. Mol. Opt. Phys. **41** (2008) 225503 (8pp) doi:10.1088/0953-4075/41/22/225503

Coherent control of magneto-optic rotation

Kanhaiya Pandey, Ajay Wasan[1] and Vasant Natarajan

Department of Physics, Indian Institute of Science, Bangalore 560 012, India

E-mail: vasant@physics.iisc.ernet.in

Received 8 August 2008, in final form 29 September 2008
Published 10 November 2008
Online at stacks.iop.org/JPhysB/41/225503

Abstract

We experimentally study the rotation of the plane of polarization of a laser beam passing through room-temperature Rb vapour. The rotation occurs because the medium behaves differently for the two orthogonally-polarized components, displaying what is known as circular birefringence or linear dichroism. The difference is induced either by a control laser applied to an auxiliary transition of a ladder-type system, or by an applied axial magnetic field. In the presence of both control laser and magnetic field, the line shape shows an interesting interplay between the two effects with regions of suppressed and enhanced rotation. The line shapes can be understood qualitatively based on a density-matrix analysis of the system.

(Some figures in this article are in colour only in the electronic version)

1. Introduction

The rotation of the plane of polarization of light by a medium in the presence of a magnetic field, generally called magneto-optical rotation (MOR), has been studied for a long time. The phenomenon arises due to the birefringence or dichroism of the medium induced by the magnetic field, and is known as the Faraday effect [1–4] when the applied magnetic field is longitudinal (causing circular birefringence) and the Voigt effect [5–7] when the field is transverse (causing linear dichroism). MOR has important applications [8] in diverse areas such as polarization control, Faraday optical isolators, magnetometry [9] and laser-frequency stabilization [10, 11]. Magneto-optical effects have also played an important role in measuring parity-violating optical activity in atoms caused by the weak interaction [12]. In recent times, another technique of optical rotation has been studied, which uses the fact that the properties of a multilevel atomic system can be 'coherently controlled' by using suitable control lasers. In such systems, the strong control laser applied on one transition induces birefringence or dichroism for a probe laser on a second transition, similar to the phenomenon of electromagnetically induced transparency (EIT) where the control laser modifies the absorption properties of the probe [13]. Coherent control of optical rotation [14–18] again has important applications, e.g. in precision measurements of parity violation in atoms [19], and polarization control in the deep UV region where standard optical elements are currently unavailable. The chirality of the optical gain induced by a control laser has also been used to measure parity violation in atoms [20]. Finally, Faraday rotation in the presence of a coupling laser has been studied recently with cold atoms in a magneto-optic trap [21].

It has been theoretically predicted that the combination of coherent control and magnetic fields for optical rotation [22–24], termed coherent control of magneto-optical rotation (CCMOR), can result in enhanced rotation and useful modifications to the line shape. In this work, we experimentally study the phenomenon of CCMOR in a ladder-type three-level system in room-temperature Rb vapour. The changes in the line shape in the presence of both the control field and the magnetic field can be explained qualitatively by a density-matrix analysis of the system. In a previous experiment demonstrating coherent control of optical rotation (i.e. without a magnetic field) in a ladder system in Rb [16], the detection method had contributions from both induced ellipticity and rotation. By contrast, we use balanced detection of both polarization components, which is a standard technique to eliminate any effects of induced ellipticity of the probe beam [18]. The measured signal is then purely due to optical rotation and the resultant line shapes are easier to understand.

[1] Present address: Department of Physics, Indian Institute of Technology, Roorkee 247 667, India.

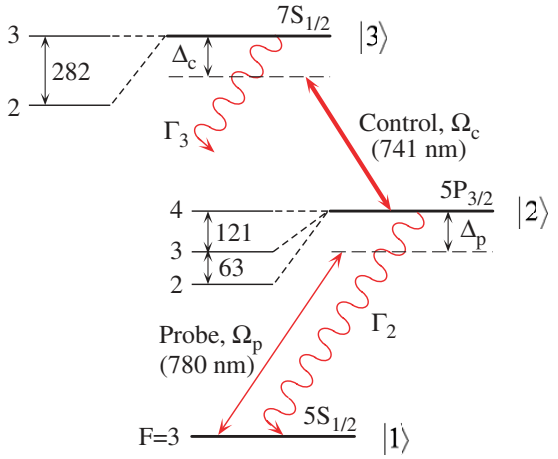

Figure 1. Three-level ladder system in ^{85}Rb. The relevant hyperfine levels in each state are shown, with intervals given in MHz.

2. Theoretical analysis

We first consider the theoretical prediction for optical rotation in a ladder system, as shown in figure 1. For specificity, we consider the $5S_{1/2} \rightarrow 5P_{3/2} \rightarrow 7S_{1/2}$ transition in ^{85}Rb. The strong control laser drives the upper $|2\rangle \leftrightarrow |3\rangle$ transition (at 741 nm) with the Rabi frequency Ω_c and detuning Δ_c, while the weak probe is scanned across the lower $|1\rangle \leftrightarrow |2\rangle$ transition (at 780 nm) with the Rabi frequency Ω_p. The decoherence rate from the $5P_{3/2}$ state is Γ_2 (= 6 MHz) while the corresponding rate from the $7S_{1/2}$ state is Γ_3 (= 11 MHz).

2.1. Circularly-polarized control

It is well known that a control laser which is circularly polarized induces circular birefringence for the probe laser, i.e., it changes the refractive index for the right- and left-circularly polarized components. This can be understood from the simplified energy-level diagram (neglecting fine-structure and hyperfine-structure effects) shown in figure 2(a). There are three sublevels for the intermediate state ($m_F = 0, \pm 1$), but only one of these levels forms a ladder system with the circularly-polarized components of the probe laser. It is this differential coupling that causes the circular birefringence. The angle of rotation for the plane of polarization of the probe laser is therefore given by

$$\theta = \frac{\alpha l}{2}[\mathrm{Re}(s^+) - \mathrm{Re}(s^-)], \tag{1}$$

where α is the absorption coefficient, l is the interaction length and s^+ (s^-) is the susceptibility for right- (left-) circularly polarized light. From the steady-state solution of the density matrix equations for this three-level system, the two susceptibilities are (to all orders in Ω_c and to first order in Ω_p) [25]

$$s^+ = \frac{\mathrm{i}\Gamma_2/2}{[\Gamma_2/2 + \mathrm{i}\Delta_p] + \frac{\Omega_c^2/4}{\Gamma_3/2 - \mathrm{i}(\Delta_p + \Delta_c)}},$$
$$s^- = \frac{\mathrm{i}\Gamma_2/2}{[\Gamma_2/2 + \mathrm{i}\Delta_p]}. \tag{2}$$

Note that the control laser also induces circular dichroism for the probe beam, i.e., different degrees of absorption for right- and left-circularly polarized components. This arises from differences in the imaginary part of the two susceptibilities and results in ellipticity of the probe beam, but does not cause rotation.

The above analysis is correct for a stationary atom. In a gas of atoms at room temperature, we have to account for the thermal velocity of moving atoms. The effect of the velocity is to change the frequency of the beams by $\pm v/\lambda$, with the sign depending on whether the atom is moving along or opposite to the light-propagation direction. The calculated rotation after accounting for the Maxwell–Boltzmann distribution of velocities is shown in figure 2(b), for $\alpha l = 25\%$, and $\Omega_c = 20$ MHz. The inset shows the real part of the susceptibility for the two circular polarizations of the probe.

Now let us consider what happens when we add an axial magnetic field B. Since the direction of the magnetic field and the direction of propagation of the control laser are the same, both cause circular birefringence. The effect of the field, as shown in figure 2(a), is to shift each magnetic sublevel by an amount $g\mu_B m B$, where g is the Landé g factor, μ_B is the Bohr magneton and m is the magnetic quantum number of the sublevel. Therefore, the two susceptibilities now become

$$s^+ = \frac{\mathrm{i}\Gamma_2/2}{[\Gamma_2/2 + \mathrm{i}(\Delta_p + g\mu_B B)] + \frac{\Omega_c^2/4}{\Gamma_3/2 - \mathrm{i}(\Delta_p + \Delta_c)}},$$
$$s^- = \frac{\mathrm{i}\Gamma_2/2}{[\Gamma_2/2 + \mathrm{i}(\Delta_p - g\mu_B B)]}. \tag{3}$$

The calculated line shape for rotation in the presence of both the control laser and magnetic field is shown in figure 2(c). The value of the field is 30 G, and again the calculation takes into account thermal averaging in room-temperature vapour.

The magnitude of optical rotation is in the range of milliradians. Since the rotation angle is directly proportional to the optical path length αl, it can be increased by several orders of magnitude by increasing the cell length and heating the cell to increase the atomic density. In Rb, increasing the cell temperature from room temperature to 90 °C increases the atomic density by more than two orders of magnitude. The magneto-optic rotation can also be increased by increasing the magnetic field strength. The coherent control rotation can be increased by increasing the Rabi frequency of the control laser. For example, a previous experiment on coherent control of optical rotation with the same ladder system in Rb used a Rabi frequency of 870 MHz and a heated vapour cell ($\alpha l = 28$) to observe a rotation of about 1 rad [16]. Theoretical calculations of CCMOR have assumed $\alpha l = 300$ to predict rotation of few radians [24]. However, even with our modest values of Rabi frequency (20 MHz) and optical path length ($\alpha l = 0.25$), we see that the control laser can enhance or suppress the magneto-optic rotation by 60% on either side of the optical resonance. Note that, for MOR applications such as magnetometry and laser-frequency stabilization, it is not the angle of rotation but the signal-to-noise ratio in measuring the angle that is important.

As mentioned earlier, the above simplified picture ignores the effects of fine-structure and hyperfine-structure

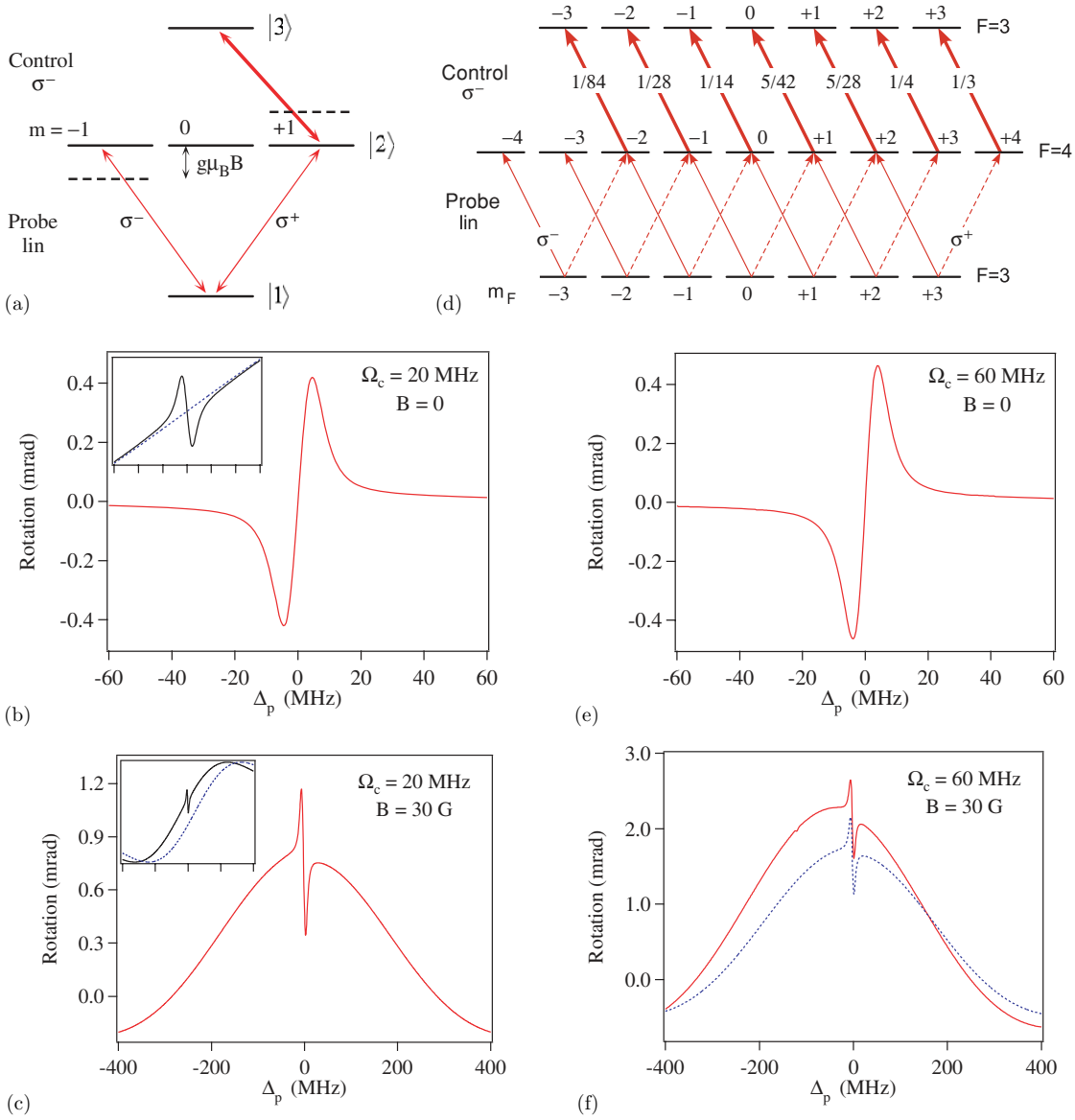

Figure 2. Optical rotation in the presence of circularly-polarized control. In (a), we show a simplified energy-level diagram without fine-structure or hyperfine-structure effects. Only one of the magnetic sublevels of the intermediate level is coupled by the two lasers. The dotted levels represent the shift in the presence of a magnetic field. In (b) and (c), we show coherent control of rotation with and without a magnetic field and $\alpha l = 0.25$. The insets (with the same x-axis) show the real part of the susceptibility for opposite circular polarizations of the probe. The energy-level diagram in (d) shows the complete sublevel structure taking into account the F value for each level, and gives the Clebsch–Gordan coefficients for the control-laser transitions. The corresponding rotation curves are shown in (e) and (f). The dotted curve in (f) is the rotation without including the additional $F = 2, 3$ hyperfine levels in the intermediate state.

interactions. This is also the procedure followed in previous work on this system [16]. A more accurate picture would incorporate the total angular momentum **F** and all the m_F sublevels for each level. The complete energy-level diagram for the main $F = 3 \rightarrow F = 4 \rightarrow F = 3$ transition is shown in figure 2(d). As before, the control laser causes circular birefringence because some of the sublevels of the intermediate level do not couple to form a ladder system. We can see that this condition would be satisfied as long as the value of F in the intermediate level is greater than or equal to that of the upper level. Thus, from the hyperfine levels shown in figure 1, there will be an additional contribution only from the $F = 3$ level of the intermediate state. The calculated rotation with the full sublevel structure is shown in figure 2(e). Since all the transitions coupled by the control laser do not contribute equally (due to the different Clebsch–Gordan coefficients), the same amount of rotation requires an increase in the Rabi frequency of the control laser to 60 MHz. Apart from this difference, the line shape is almost identical to that shown in (b), which is calculated from the simplified picture. In addition, the contribution of the $F = 3$ hyperfine level of the intermediate state is negligible, and the rotation calculated with and without this level shows no difference. This is because the $F = 3$ level is 121 MHz lower [26], and the ac Stark shift of the detuned level is ten times smaller. Indeed, EIT experiments on this ladder system show a single transparency dip from the resonant $F = 4$ level, and no additional dip due to the off-resonant $F = 3$ level [27].

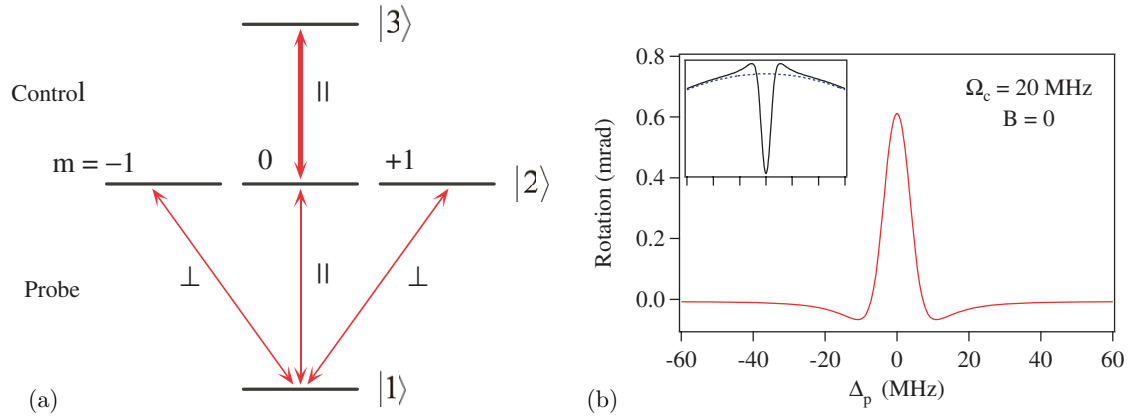

Figure 3. Optical rotation in the presence of linearly-polarized control. In (a), we show the magnetic sublevels coupled by the two lasers for $\beta = 45^\circ$, inducing linear dichroism. In (b), we show coherent control of rotation for the probe polarization. The inset (with the same x-axis) shows the imaginary part of the susceptibility for parallel and perpendicular linear polarizations.

In the presence of a magnetic field, the shift of a hyperfine level is given by $g_F \mu_B m_F B$, with different Landé g_F's for each level. The calculated line shape in the presence of both the control laser and a magnetic field is shown in figure 2(f). The other hyperfine levels of the intermediate state are also included since they contribute to the Faraday rotation, though not to the coherent-control part. The effect of the additional hyperfine levels is to cause an asymmetry in the line shape. When these levels are not included, the line shape is similar to the simplified calculation shown in (c).

Therefore, in the following, we use the simplified picture for our calculations, with the understanding that the presence of the other hyperfine levels results in some asymmetry of the line shape.

2.2. *Linearly-polarized control*

In the presence of a control laser which is linearly polarized, it is the linear dichroism induced in the medium that is responsible for the rotation of the plane of polarization of the probe beam, similar to what happens in the Voigt effect. In other words, the differential absorption of parallel and perpendicular polarization components of the probe results in the rotation. The rotation angle is therefore related to the imaginary part of the susceptibility and is given by

$$\theta = \frac{\alpha l}{2} \sin(2\beta)[\mathrm{Im}(s_\parallel) - \mathrm{Im}(s_\perp)], \tag{4}$$

where β is the angle between the planes of polarization of the control laser and the incoming probe beam, and $\parallel$ and $\perp$ are defined with respect to the control. The magnetic sublevels coupled by the probe and control lasers for $\beta = 45^\circ$ are shown in figure 3(a). Note how only the $m = 0$ sublevel of the intermediate state forms a ladder system.

As before, the density-matrix analysis yields

$$s_\parallel = \frac{\mathrm{i}\Gamma_2/2}{(\Gamma_2/2 + \mathrm{i}\Delta_p) + \frac{\Omega_c^2/4}{\Gamma_3/2 - \mathrm{i}(\Delta_p + \Delta_c)}}, \qquad s_\perp = \frac{\mathrm{i}\Gamma_2/2}{(\Gamma_2/2 + \mathrm{i}\Delta_p)}. \tag{5}$$

The calculated line shape in room-temperature vapour for $\beta = 45^\circ$ and $\Omega_c = 20$ MHz is shown in figure 3(b). Note again that the linear birefringence induced in the medium (arising from the real part of the susceptibilities) causes ellipticity but no rotation.

The addition of an axial magnetic field complicates matters because the rotation is an interplay between the linear dichroism induced by the control and the circular birefringence induced by the B field. In other words, the linear-dichroism axis of the control laser will precess around the magnetic-field axis, which will become significant when the field is strong enough. However, it is possible to calculate the rotation when the control and probe are polarized parallel to each other, i.e. $\beta = 0^\circ$. Under these conditions, equation (4) shows that there is no rotation in the presence of the control laser alone. But there will be rotation when an axial B field is present due to the circular birefringence induced by the field, now modified by the presence of the linearly polarized control laser. As seen from the energy levels in figure 4(a), both the $m = -1$ and $m = +1$ sublevels form ladder systems, but the magnetic field shifts them in opposite directions. The rotation angle is therefore

$$\theta = \frac{\alpha l}{2}[\mathrm{Re}(s^+) - \mathrm{Re}(s^-)], \tag{6}$$

with the susceptibilities given by

$$s^\pm = \frac{\mathrm{i}\Gamma_2/2}{[\Gamma_2/2 + \mathrm{i}(\Delta_p \pm g\mu_B B)] + \frac{\Omega_c^2/4}{\Gamma_3/2 - \mathrm{i}(\Delta_p + \Delta_c)}}. \tag{7}$$

The calculated line shape in room-temperature vapour with a 30 G field is shown in figure 4(b). The real part of the susceptibility for the two circular components (shown in the inset) has the same line shape but is pulled in different directions by the magnetic field. The rotation is therefore strongly suppressed by the control laser on resonance.

3. Results and discussion

We now turn to the experimental confirmation of these predicted line shapes. The experiments were done in a room-temperature Rb vapour cell, as shown schematically in figure 5.

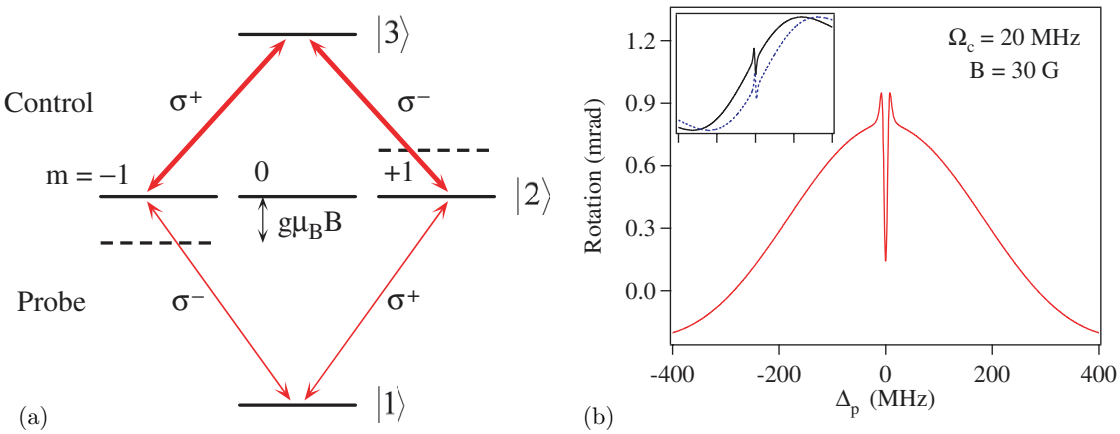

Figure 4. CCMOR with linearly-polarized control and a magnetic field. In (a), we show the magnetic sublevels coupled by the two lasers for $\beta = 0°$, and the circular birefringence in the presence of a magnetic field due to the opposite energy shifts of the sublevels. In (b) we show control of magneto-optic rotation for $B = 30$ G. The inset (with the same x-axis) shows the real part of the susceptibility for opposite circular polarizations.

The probe beam was derived from a feedback-stabilized diode laser system operating on the D_2 line at 780 nm [28]. The linewidth of the laser after stabilization was around 500 kHz. It was scanned across the $5S_{1/2}(F = 3) \rightarrow 5P_{3/2}(F = 2, 3, 4)$ hyperfine transitions of ^{85}Rb. Note that the $F = 2$ hyperfine level of the ground state is 3 GHz away, and does not play a role in the experiment. The size of the probe beam was about 2.5 mm and its power was 50 μW. It was linearly polarized and the angle of rotation after passing through the cell was determined by first splitting it into its two orthogonal components (using a polarizing beam splitter cube with an extinction ratio of 1000:1) and then measuring the power in each component. This kind of balanced detection [18] gives the rotation angle independent of any induced ellipticity in the beam. The counter-propagating control beam came from a ring-cavity Ti:sapphire laser (Coherent 899-21) tuned to 741 nm. The laser was stabilized to an ovenized reference cavity that gave it a linewidth of 500 kHz. It was kept on the $5P_{3/2}(F = 4) \rightarrow 7S_{1/2}(F = 3)$ hyperfine transition in ^{85}Rb. The control beam had a diameter of 4 mm and its power was varied from 100 to 350 mW. The on-resonance absorption of the probe beam (in the absence of the control beam) through the 5 cm long vapour cell was 25%. It had a 30 cm long solenoid coil wound around it so as to produce a uniform magnetic field of up to 30 G.

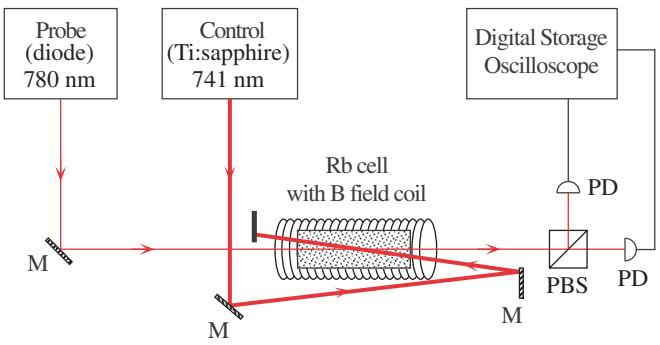

Figure 5. Schematic of the experiment. The angle between the beams in the vapour cell has been exaggerated for clarity, in reality it is less than 10 mrad. Figure key: M, mirror; PBS, polarizing beam splitter; PD, photodiode.

3.1. Circularly-polarized control

For the first set of experiments, we used a control beam which was circularly polarized and had power of 210 mW. We first measured probe rotation in the absence of a magnetic field. The results are shown in figure 6(a). The primary peak is a dispersive peak showing a line shape similar to the calculated one in figure 2(a), with a maximum rotation of 1.5 mrad. However, there is a second smaller peak of 282 MHz to the left that has a different (non-dispersive) line shape. This is due to the $F = 2$ hyperfine level of the upper state, from which the control laser is detuned by +282 MHz. Thus the two-photon resonance condition will be satisfied only when the probe is detuned by -282 MHz. The effect of this additional hyperfine level is also seen in EIT experiments, and can be used for high-resolution hyperfine spectroscopy of excited states, as shown by us in earlier work [29]. The detuning has a significant effect on the line shape of rotation, as seen in figure 6(b). Note the progressive increase in the lower lobe compared to the upper one as the control is increasingly detuned to the blue.

The combined effect of the control laser and the magnetic field (CCMOR) is shown in figure 7, for control power of 210 mW and three values of the magnetic field. The line shape agrees qualitatively with our theoretical prediction with the appearance of a dispersive region near the peak of the Doppler-broadened curve. The change in rotation due to the control laser is $\pm 75\%$ at the line centre for a field of 10 G. But the effect becomes progressively smaller as the field strength is increased, and reduces to $\pm 10\%$ at 30 G. The asymmetry in the line shape is due to the presence of the additional hyperfine levels of the intermediate state, which is also seen in the calculated line shape (shown in figure 2(f)) when these levels are included. However, there is a difference between the widths of the upper and lower lobes, which is not seen in the calculation.

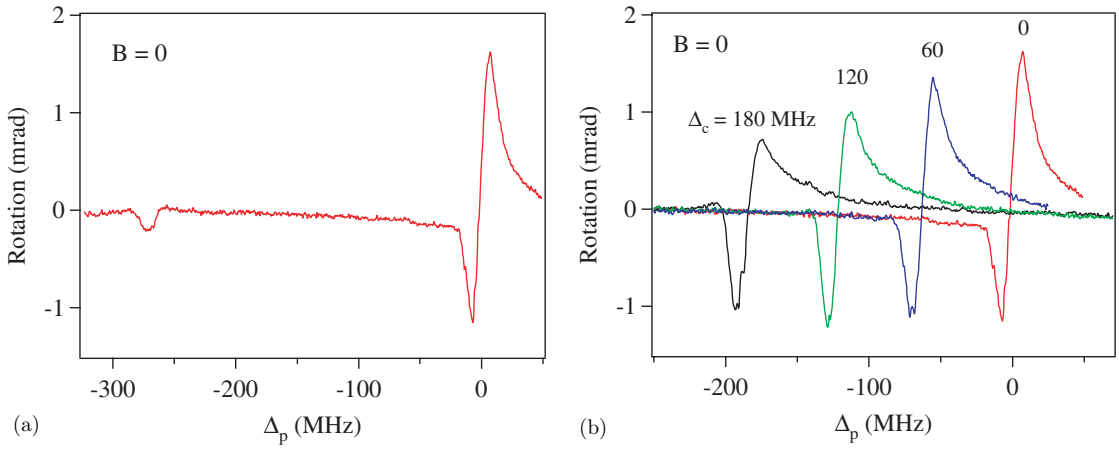

Figure 6. Measured rotation in the presence of a control laser that is circularly polarized and no magnetic field in ^{85}Rb. The dip on the left in (a) is due to the $F = 2$ hyperfine level of the $7S_{1/2}$ state, from which the control laser is detuned by +282 MHz. The effect of detuning on the line shape is seen in (b).

3.2. Linearly-polarized control

The next set of experiments was done with a control laser which was linearly polarized at an angle of 45° (from the probe beam), and no magnetic field. The power in the beam was 280 mW. The rotation, shown in figure 8, agrees with the predicted line shape. As in the previous case, there is a second peak of 282 MHz to the left due to the presence of the detuned hyperfine level. The line shape of the second peak is again different because detuning the control affects the line shape, as seen from the curve measured with +50 MHz detuning.

Another striking feature of the rotation curve is that it becomes negative on either side of the resonance, seen in both the calculation and measurement. In EIT, this would correspond to increased absorption on either side of the transparency dip. Such a line shape has been predicted by us in earlier work with EIT in this ladder system [29]. It arises due to thermal averaging in room-temperature vapour; the different wavelengths of the control and probe lasers imply that the Doppler shifts (which depend on the thermal velocity of the atom) for the two beams are different. However, observing this kind of line shape in EIT is difficult because of other broadening mechanisms. It has been observed only recently for EIT with Rydberg atoms [30] and has not been observed previously in optical rotation.

The other important effect is to see the modification to the line shape in the presence of a magnetic field, as shown in figure 9. With $\beta = 0°$, the curve in (a) shows that the control laser causes a reduction in rotation by 40% at line centre, as predicted in figure 3(b). There is a slight asymmetry in the observed line shape, which is again due to the presence of the other hyperfine levels that are not included in the calculation. In addition, the width of the observed dip at the line centre is larger than the calculated one. This is probably because of a misalignment angle between the control and probe beams. In EIT, even a small misalignment angle of a few milliradians has been shown to cause a significant increase in the linewidth [31].

As discussed in the theoretical section, with $\beta = 45°$, there is a competition between the linear dichroism induced

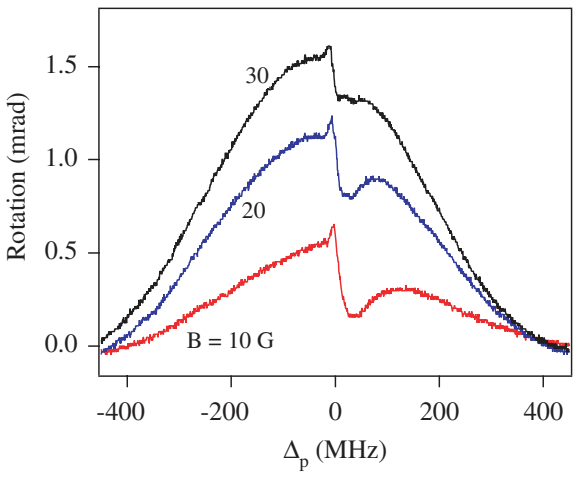

Figure 7. Measured rotation in the presence of a control laser that is circularly polarized and three values of magnetic field.

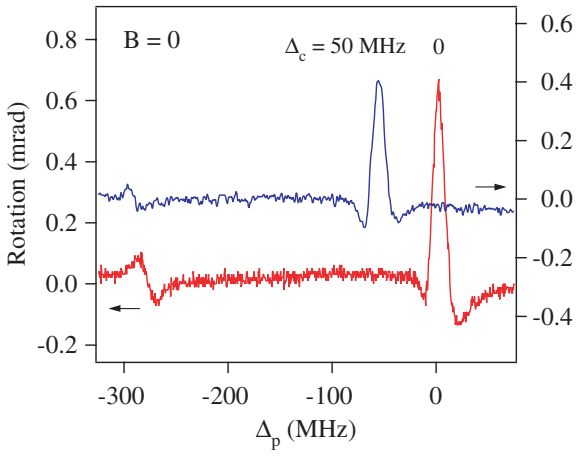

Figure 8. Measured rotation in the presence of a control laser which is linearly polarized (with $\beta = 45°$) and no magnetic field, for two values of control detuning. The right axis is for the curve with $\Delta_c = 50$ MHz.

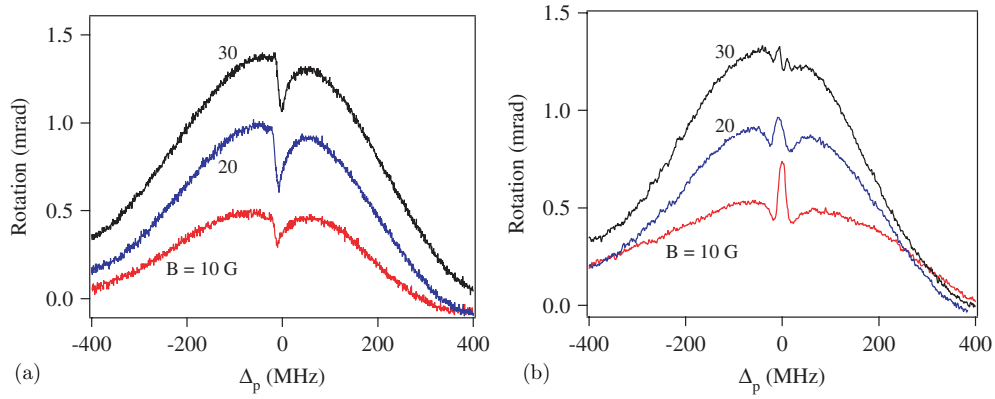

Figure 9. Measured rotation in the presence of a control laser which is linearly polarized and three values of magnetic field. $\beta = 0^\circ$ for (a) and $\beta = 45^\circ$ for (b).

by the control laser and the circular birefringence induced by the magnetic field. This competition is seen in the measured curves shown in figure 9(b). As the field is increased, the effect of the control is reduced progressively. Thus, for $B = 10$ G, the control laser dominates near the line centre and increases the MOR effect by 40%. But by the time the field reaches a value of 30 G, the effect of the control becomes negligible.

4. Conclusion

In summary, we have studied the effect of a near-resonant control laser on magneto-optic rotation through room-temperature Rb vapour. In the absence of a magnetic field, the rotation of the probe beam shows a dispersive line shape when the control laser is circularly polarized; and a peak with regions of negative rotation on either side when the control laser is linearly polarized (at 45° to the probe). When an axial magnetic field is added, the control laser causes significant modification to the line shape near resonance, which can be used to control the amount of rotation in MOR applications. The combined effect, called coherent control of magneto-optic rotation, can be understood qualitatively from a density-matrix analysis of a simplified three-level system that neglects fine and hyperfine-structure effects. The calculated line shapes agree with the measured ones when the control laser is either circularly polarized or linearly polarized at 0° to the probe. However, in the presence of a linearly-polarized control at 45°, there is a competition between the linear dichroism induced by the control laser (related to differential absorption and hence the imaginary part of the susceptibility) and the circular birefringence induced by the magnetic field (related to differential phase change and hence the real part of the susceptibility). The experimental results show that the effects of the control laser dominate at the line centre for a field of 10 G and become negligible when the field increases to 30 G.

Acknowledgments

This work was supported by the Department of Science and Technology, India. One of us (VN) acknowledges support from the Homi Bhabha Fellowship Council and the others (KP, AW) acknowledge financial support from the Council of Scientific and Industrial Research, India.

References

[1] Faraday M 1855 *Exp. Res.* **3** 2164
[2] Kristensen M, Blok F J, van Eijkelenborg M A, Nienhuis G and Woerdman J P 1995 Onset of a collisional modification of the Faraday effect in a high-density atomic gas *Phys. Rev.* A **51** 1085–96
[3] Labeyrie G, Miniatura C and Kaiser R 2001 Large Faraday rotation of resonant light in a cold atomic cloud *Phys. Rev.* A **64** 033402
[4] Franke-Arnold S, Arndt M and Zeilinger A 2001 Magneto-optical effects with cold lithium atoms *J. Phys. B: At. Mol. Opt. Phys.* **31** 2527–36
[5] Macaluso D and Corbino O M 1898 *Nuovo Cimento* **8** 257
[6] Yamamoto M and Murayama S 1979 *J. Opt. Soc. Am.* **69** 781
[7] Schuller F, Macpherson M J D, Stacey D N, Warrington R B and Zetie K P 1991 The voigt effect in a dilute atomic vapour *Opt. Commun.* **86** 123–7
[8] Budker D, Gawlik W, Kimball D F, Rochester S M, Yashchuk V V and Weis A 2002 Resonant nonlinear magneto-optical effects in atoms *Rev. Mod. Phys.* **74** 1153–201
[9] Edwards N H, Phipp S J and Baird P E G 1995 Magneto-optic rotation for an arbitrary field direction *Europhys. Lett.* **28** 4041–54
[10] Cyr N and Têtu M 1991 Solitary resonance in the velocity-selective magnetic-optical activity spectrum of the 87rb d2 line *Opt. Lett.* **16** 946–8
[11] Yashchuk V V, Budker D and Davis J R 2000 Laser frequency stabilization using linear magneto-optics *Rev. Sci. Instrum.* **71** 341–6
[12] Bouchiat M-A and Bouchiat C 1997 Parity violation in atoms *Rep. Prog. Phys.* **60** 1351–96
[13] Harris S E 1997 Electromagnetically induced transparency *Phys. Today* **50** 36–9
[14] Liao P F and Bjorklund G C 1976 Polarization rotation induced by resonant two-photon dispersion *Phys. Rev. Lett.* **36** 584–7
[15] Pavone F S, Bianchini G, Cataliotti F S, Hänsch T W and Inguscio M 1997 Birefringence in electromagnetically induced transparency *Opt. Lett.* **22** 736–8
[16] Wielandy S and Gaeta A L 1998 Coherent control of the polarization of an optical field *Phys. Rev. Lett.* **81** 3359–62
[17] Yoon T H, Park C Y and Park S J 2004 Laser-induced birefringence in a wavelength-mismatched cascade system

of inhomogeneously broadened Yb atoms *Phys. Rev.* A **70** 061803

[18] Wang B, Li S, Ma J, Wang H, Peng K C and Xiao M 2006 Controlling the polarization rotation of an optical field via asymmetry in electromagnetically induced transparency *Phys. Rev.* A **73** 051801

[19] Cronin A D, Warrington R B, Lamoreaux S K and Fortson E N 1998 Studies of electromagnetically induced transparency in thallium vapour and possible utility for measuring atomic parity nonconservation *Phys. Rev. Lett.* **80** 3719–22

[20] Guéna J, Chauvat D, Jacquier P, Jahier E, Lintz M, Sanguinetti S, Wasan A, Bouchiat M A, Papoyan A V and Sarkisyan D 2003 New manifestation of atomic parity violation in cesium: a chiral optical gain induced by linearly polarized 6s–7s excitation *Phys. Rev. Lett.* **90** 143001

[21] Choi J M, Kim J M and Cho D 2007 Faraday rotation assisted by linearly polarized light *Phys. Rev.* A **76** 053802

[22] Fleischhauer M and Scully M O 1994 Quantum sensitivity limits of an optical magnetometer based on atomic phase coherence *Phys. Rev.* A **49** 1973–86

[23] Patnaik A K and Agrawal G S 2000 Laser field induced birefringence and enhancement of magneto-optical rotation *Opt. Commun.* **179** 97–106

[24] Patnaik A K and Agrawal G S 2001 Coherent control of magneto-optical rotation in homogeneously broadened medium *Opt. Commun.* **199** 127–42

[25] Gea-Banacloche Julio, Li Y Q, Jin S Z and Xiao M 1995 Electromagnetically induced transparency in ladder-type inhomogeneously broadened media: theory and experiment *Phys. Rev.* A **51** 576–84

[26] Rapol U D, Krishna A and Natarajan V 2003 Precise measurement of the hyperfine structure in the $5P_{3/2}$ state of ^{85}Rb *Eur. Phys. J.* D **23** 185–8

[27] Pandey K and Natarajan V 2008 Splitting of electromagnetically induced transparency under strong-probe conditions due to doppler averaging *J. Phys. B: At. Mol. Opt. Phys.* **41** 185504 (4pp)

[28] Banerjee A, Rapol U D, Wasan A and Natarajan V 2001 High-accuracy wavemeter based on a stabilized diode laser *Appl. Phys. Lett.* **79** 2139–41

[29] Krishna A, Pandey K, Wasan A and Natarajan V 2005 High-resolution hyperfine spectroscopy of excited states using electromagnetically induced transparency *Europhys. Lett.* **72** 221–7

[30] Mohapatra A K, Jackson T R and Adams C S 2007 Coherent optical detection of highly excited Rydberg states using electromagnetically induced transparency *Phys. Rev. Lett.* **98** 113003

[31] Carvalho P R S, de Araujo Luis E E and Tabosa J W R 2004 Angular dependence of an electromagnetically induced transparency resonance in a Doppler-broadened atomic vapor *Phys. Rev.* A **70** 063818